Combustion and Flame 274 (2025) 113978

Contents lists available at ScienceDirect

Combustion and Flame

journal homepage: www.sciencedirect.com/journal/combustion-and-flame

Sensitizing effect of acetylene and 1,3-butadiene on toluene oxidation in laminar flames

Ewald Keksel [a], Sebastian Kluge [a], Domenik Schleier [a], Martin Höner [a], Yasin Karakaya [a], Thomas Bierkandt [b], Markus Köhler [b], Tina Kasper [a,*]

[a] Technical Thermodynamics, Paderborn University, Paderborn, Germany
[b] Institute of Combustion Technology, German Aerospace Center (DLR), Stuttgart, Germany

ARTICLE INFO

Keywords:
PEPICO spectroscopy
Toluene oxidation
Low-temperature
Fuel surrogate
Sensitization

ABSTRACT

Fuel surrogates are composed of a limited number of different hydrocarbons and designed to mimic the combustion properties of real-world fuels. Toluene is often a major component of such surrogates. Consequently, the main oxidation pathways of toluene have been investigated intensively and many reaction mechanisms are available in the literature. Here, major intermediates of toluene consumption in low-pressure laminar flames are identified by comparison with mass-resolved threshold photoelectron spectra measured by photo electron photoion coincidence spectroscopy at the Swiss Light Source. The measurements confirm the main consumption pathways of toluene in the literature. In fuel surrogates, the oxidation chemistry of toluene interacts with the oxidation chemistry of other hydrocarbons in the mixture. The interaction is particularly important in the flame front where the fuel is consumed at low temperatures and fuel conversion is initiated. In toluene flames doped with 1,3-butadiene or acetylene investigated here, an acceleration of toluene conversion by the low-temperature reactions of the additive is observed experimentally for both flames. The observations are explained by simulations of the flame. For 1,3-butadiene, typical low-temperature oxidation reactions, e.g., the formation of peroxide intermediates, form small flame radicals that play an important role for the acceleration. For acetylene, hydrogen-addition to the fuel leads to the formation of vinyl radicals and the subsequent oxidation sequences of the vinyl radicals release further small radicals. The oxidation of acetylene also increases the temperature and accelerates toluene consumption at an earlier stage in the flame than without acetylene. Remarkable and counterintuitive for the design of fuel surrogates is the fact that the acceleration mechanism of acetylene seems to be more effective than that of 1,3-butadiene, which is reflected in faster toluene consumption in the acetylene/toluene flame front than in the 1,3-butadiene/toluene flame front, while a neat toluene flame shows the slowest consumption of toluene.

1. Introduction

Although renewables are increasingly used, advanced combustion strategies in engines serve as a transitional technology in challenging areas for electrification, such as heavy-duty machinery and the maritime and aviation sectors. Engines operated with techniques like Gasoline-Controlled Auto-Ignition (GCAI) and Premixed Charge Compression Ignition (PCCI) burn fuel-lean, premixed, homogeneous fuel-air mixtures and have the benefit of producing less soot and nitrogen oxides [1,2]. Controlling the ignition in such engines during load transients is challenging due to significant fluctuations in temperature, mixture composition, and pressure from cycle to cycle and within a cycle [1].

To address the issue of ignition, a detailed understanding of the involved chemical kinetics is crucial, but the chemical complexity of conventional real-world diesel and gasoline fuels is too large to understand the interactions of any two of its components in detail. Consequently, surrogate fuels or simple fuel mixtures are used for such investigations. They are designed to mimic physical and chemical characteristics of complex fuels [3].

Toluene is used frequently as a representative aromatic component of surrogate fuels [3]. This is one reason why toluene kinetics have been investigated in detail in the context of reference fuels, e.g., [3,4] or in fundamental kinetics studies, e.g., [5–7]. Numerous experimental data are available including global parameters like laminar burning velocity

* Corresponding author.
E-mail address: tina.kasper@upb.de (T. Kasper).

https://doi.org/10.1016/j.combustflame.2025.113978
Received 9 September 2024; Received in revised form 7 January 2025; Accepted 8 January 2025
Available online 23 January 2025

[8], ignition delay time [9] and speciation data in jet-stirred [5,10] and flow reactors [5,11], premixed flames [12,13] and shock tubes [7,14]. In these studies, the experiments have served to provide validation data for the reported reaction mechanisms.

Acetylene and 1,3-butadiene are often formed as intermediates from larger fuels [7]. They can be expected to be present in fuel mixtures in engines after an intermediate compression stroke or if the fuel is injected in pulses. Both techniques are established for ignition timing control in engines that rely on chemically controlled ignition [1,2]. Consequently, the interaction of toluene and acetylene as well as toluene and 1,3-butadiene at low temperature is of specific interest when chemical reactions during ignition are to be described. The interaction at comparatively low temperatures was studied here in the flame front of low-pressure premixed toluene-acetylene and toluene-butadiene flames. Measurements were performed by flame-sampling photoionization molecular-beam mass spectrometry with photo electron photoion coincidence spectroscopy (PEPICO) using vacuum ultraviolet (VUV) light generated at the Swiss Light Source (SLS).

The kinetics of acetylene and 1,3-butadiene combustion have also been investigated intensively and reviewed recently in [15,16] and [17], respectively. In summary, the ignition delay times (IDT) of toluene, acetylene and 1,3-butadiene differ substantially. At unit equivalence ratio, 1200 K, 20 bar and similar dilutions, toluene has an IDT of ca. 0.2 ms [14], acetylene has an IDT of ca. 0.02 ms [16] and 1,3-butadiene has an IDT of ca. 0.0001 ms [18]. 1,3-butadiene is the only of these three fuels which unambiguously exhibits typical low-temperature chemistry such as the formation of peroxide intermediates [17,18], resulting for example in an inflection in the IDT curves and negative temperature coefficient (NTC) behavior at other reaction conditions. For acetylene, low temperature chemistry is not reported, e.g., acetylene IDT show Arrhenius behavior at all temperatures, with no NTC at low to intermediate temperatures [16]. The model of Yuan et al. [5,14] predicts NTC behavior and consequently some low-temperature chemistry for toluene. Because of the very limited reactivity of toluene at low temperatures few experimental data exist below 1000 K.

The interaction of acetylene with toluene in fuel mixtures has attracted attention mostly in the context of polyaromatic hydrocarbon formation and has been studied under pyrolysis conditions [7,11]. In both studies an accelerating effect of acetylene on the conversion of toluene is observed and explained by the production of H radicals through a reaction of the benzyl radical with C_2H_2 or C_2H_x intermediates. To our knowledge the interaction of toluene and 1,3-butadiene pyrolysis or oxidation have not been studied explicitly. When blending a less reactive fuel like toluene with a more reactive fuel like 1,3-butadiene typically an accelerating effect can be expected under various experimental conditions. For example, when adding 1,3-butadiene to methane flames [19], the methane conversion is accelerated. Toluene conversion is also promoted by adding more reactive components to a mixture, e.g., n-butanol [20] or typical reference fuel components like n-heptane and i-octane [21].

In our own work in high-pressure flow reactors, we found a promoting effect of additives such as dimethyl ether or n-heptane on methane conversion [22,23]. Based on this work we expected an accelerating effect which increases with fuel reactivity, i.e., the more pronounced the low-temperature chemistry of a fuel the stronger the sensitizing effect on the less reactive fuel. Consequently, the observation that acetylene addition to low pressure toluene flames results in a stronger increase in toluene consumption in the flame front than the addition of 1,3-butadiene was surprising and is explained in the present work.

2. Experimental section

2.1. Experiment and flame conditions

The setup of the flame experiments at the SLS and the data reduction procedures are described in detail in previous work, e.g., [24] and [25]. Only the most relevant aspects are summarized here.

The flow conditions of the flames are summarized in Table 1. The equivalence ratio of 1.8 was chosen to reflect the fuel-rich conditions, that occur during regulating interventions in HCCI engines. For example, intermediate compression strokes lead to moderate increases in pressure and temperature, so that the following reactions which lead to ignition often occur in the low-temperature combustion regime. If the fuel is injected in pulses particularly fuel-rich mixtures are formed and react also at moderate temperatures.

The total volume flow of each flame had to be adjusted to keep the equivalence ratio and the C/H ratio close-to constant in all flames. In the doped flames toluene-bound carbon was reduced by the amount of dopant-bound (i.e. acetylene and 1,3-butadiene) carbon that was added. Liquid toluene is metered by an HPLC pump, vaporized, and mixed with the argon as carrier gas in a home-made vaporizer. All gases are metered by mass flow controllers and mixed with the toluene/argon stream in a heated line close to the burner. The C_7H_8/O_2/Ar flat flames are stabilized on a 6 cm diameter matrix burner at a low pressure of 60 mbar. The flames are sampled through an orifice in a quartz probe. A rapid reduction in pressure impedes further reactions in the gas sample and results in the formation of a molecular beam. The beam is skimmed and crosses the VUV-photon beam in the ionization volume of the PEPICO spectrometer. The mass resolution of the spectrometer is $m/\Delta m \approx 200$. The iPEPICO detection scheme allows the measurement of photoionization mass spectra in coincidence with velocity mapped photoelectron images, permitting to measure mass-selected threshold photoelectron spectra (ms-TPES). The ms-TPES reflect unique state-specific transitions and provide a fingerprint of the molecules with a resolution that surpasses the resolution of photoionization efficiency (PIE) curves [25]. Species identification is achieved by comparison of measured ionization energies, PIE curves, ms-TPES or Franck-Condon simulations of expected intermediates with literature data.

Following the data reduction procedures developed by Cool et al. [26] and adapted by Osswald et al. [24] and Bierkandt et al. [25] to the SLS system, the ion signals are used to obtain the main species profiles discussed here with a 10% uncertainty. Burner scans are obtained at several photon energies (in eV): 16.20, 14.35, 13.55, 12.30, 11.45, 10.60, 9.60, 9.10, 8.70, 8.30, and 7.95. Energy scans are recorded in the photon energy range of 7.0 eV to 9.7 eV (flames B, C) and 7.0 eV to 8.6 eV (flame A).

The temperature profiles for flames A–C are measured with SiO_2-coated thermocouples and radiation-corrected. The temperature profiles are determined without the influence of the sampling-probe. The influence of the sampling probe on the mole fraction profiles is due to a suction effect and cooling. Both aspects were intensively investigated by Karakaya et al. [27] and can explain the deviations between simulations and experiments near the burner surface.

2.2. Simulation

Two reaction mechanisms were used to simulate all flames. This requires that the reaction mechanisms can reproduce the conversion of all three fuels correctly.

The mechanism by Yuan et al. [5] was utilized without modifications

Table 1
Flame Conditions.

Flame	A	B	C
ϕ	1.8	1.8	1.8
C/H ratio	0.875	0.887	0.841
C_7H_8 [sccm]	164	142	142
C_4H_6 [sccm]	0	36	0
C_2H_2 [sccm]	62	0	0
O_2 [sccm]	830	822	814
Ar [sccm]	1000	1000	1000

for modeling the main species mole fraction profiles. This mechanism builds upon the initial mechanism by Zhang et al. [28] and encompasses both low-temperature and high-temperature chemistry of toluene and other hydrocarbons. It includes 272 species and 1698 reactions and was tested in a wide range of temperatures and pressures. It has been validated through numerous flame and reactor experiments, thus reliably covering a wide range of combustion parameters. This model is expected to be well-suited for investigating the chemistry in our toluene, toluene/acetylene and toluene/butadiene flames. This mechanism is chosen because it was used by the original authors in a recent study of the co-pyrolysis [11] of toluene and acetylene that also detected an accelerating effect.

The second reaction mechanism by Shao et al. [6] was developed for toluene primary reference fuels (TPRF). It builds on the broadly validated Kaust model for TPRF [29] and contains an improved model for polycyclic aromatic hydrocarbons. It performed well for all fuels contained in our simulations.

The inlet conditions from Table 1 and flame temperatures are used as boundary conditions in the simulation setup. The pressure in the reactor chamber is kept constant at 60 mbar. Simulations were performed with the laminar flame model of Ansys Chemkin 2023 R2.

3. Results and discussion

3.1. Main species profiles

The measured and simulated profiles of the main species are shown in Fig. 1a–c. The simulations using both mechanisms (Yuan et al. [5], Shao et al. [6]) capture the mole fractions in the exhaust gas of all flames very well. The profiles are shifted by 1.5 mm closer to the burner in each flame to account for differences in the setpoint of the origin between the mass spectrometric and temperature measurements. The simulations with both mechanisms are very close to each other for the main species as can be seen from Fig 1. The profiles of the simulations with the Shao et al. [6] mechanism are slightly closer to the burner (for example by about 0.03 mm for the toluene profile), indicating slightly higher reactivity. Compared to the deviations between experiments and simulations this difference is irrelevant. Deviations between simulation and

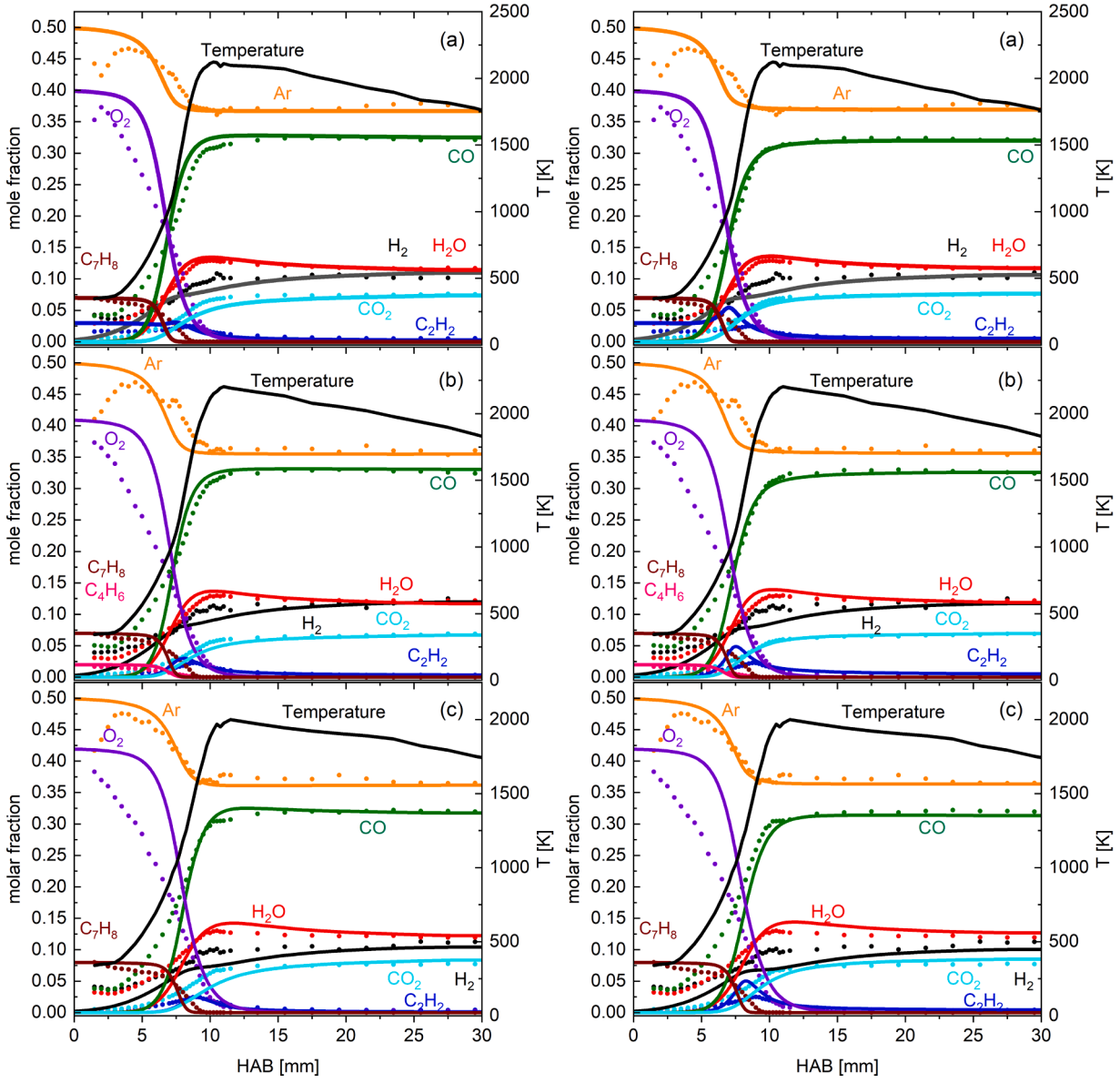

Fig. 1. Main species mole fraction profiles in Flame A-C. Symbols represent experimental data and lines the simulation. The experimentally measured temperature is plotted as the black line on the right axis.

measurement are observed in the flame front close to the burner. These are the result of using the experimentally determined temperature profiles as simulation input. Disturbances can be attributed to suction and cooling by the probe [27]. For example, the first 3 points of every argon profile drop in intensity. This can be explained by the disturbed flow field when burner and probe are very close to each other. The effect is unusually visible here, because the stand-off distance of the flames is very large. Here, this effect has no influence on the interpretation of the results because we compare species profiles that were measured with the same setup under very similar conditions, so that the disturbances are also very similar. The uncertainty of the position measurement is less than 0.5 mm in these experiments.

The temperature profiles are also very similar in Flames A–C. Flame B with 1,3-butadiene addition reaches a slightly higher maximum temperature of 2200 K compared to Flame C with a maximum temperature of 2000 K. Flame A with acetylene addition exhibits a steeper increase of the temperature profile compared to Flames B and C and reaches its maximum temperature of 2100 K about 1 mm closer to the burner. The observed order of the temperature maxima hints at different heat release in the flame front initiated by fuel conversion. In agreement with the differences in the temperature profiles, toluene is completely consumed at HAB=7 mm in Flame A, while in Flames B and C it is completely converted at HAB=8mm.

In summary, we consider the agreement between experiment and simulation as sufficient and will use both mechanisms to analyze the accelerating effect of acetylene and 1,3-butadiene on the toluene consumption.

3.2. Relative toluene consumption

The differences in toluene consumption are visualized in Fig. 2. It shows the toluene profiles in Flames A-C and the acetylene profile and the 1,3-butadiene profile from Flames A and B, respectively. All profiles are normalized to the value at HAB=2.5 mm to aid the comparison.

The steeper decrease of toluene to the baseline in Flame A (acetylene doped) implies a faster conversion of toluene than in Flame B (1,3-butadiene doped) and Flame C (undoped). The acetylene profile in Flame A shows only a very slight decrease near HAB=2 mm before it starts to increase towards larger HAB due to acetylene formation from the toluene conversion. As expected from the literature, 1,3-butadiene is the most reactive fuel, indicated by the steepest decrease in mole fraction in the flame front of Flame B.

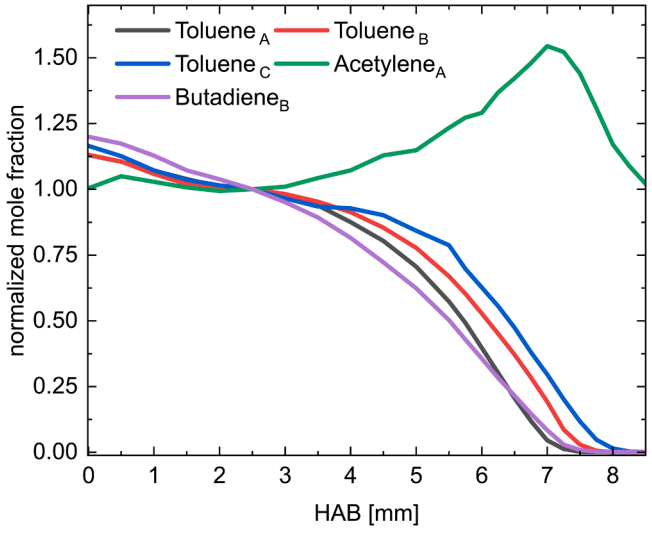

Fig. 2. Experimental fuel profiles in Flames A-C: normalized toluene mole fraction profiles in Flames A-C, acetylene profile in Flame A and 1,3-butadiene profile in Flame B. To aid visibility the experimental data are plotted as lines.

However, the observation that acetylene addition is more effective in activating toluene decomposition than 1,3-butadiene addition is not immediately comprehensible because acetylene does not exhibit low temperature chemistry.

3.3. Reaction path analysis of toluene and experimentally detected intermediates

A reaction path analysis at HAB=6.5 mm provides insights into toluene consumption. At this position in all flames about half of the initial toluene is consumed. The reaction path analysis is shown in Fig. 3 for Flame A, Fig. 4 for Flame B, Fig. 5 for Flame C.

The main reaction pathways of toluene consumption remain the same for all flames at this position, however, but the percentages of carbon flux differ as can be seen from Figs. 3-5. The addition of acetylene and 1,3-butadiene increases the carbon flux for the initial hydrogen abstraction reactions from toluene and consequently also all subsequent reactions, indicating higher reactivity. The Shao et al. [6] mechanism overall predicts a stronger increase in toluene conversion than the Yuan et al. [5] mechanism.

The main decomposition pathway of toluene in the simulation with the mechanism of Yuan et al. [5] is the formation of benzyl radicals after hydrogen abstraction by predominantly H atoms. The benzyl is converted to phenyl radicals either by oxidation via benzaldehyde or by methyl addition and subsequent elimination of ethylene. Further oxidation leads to phenyloxy radicals which are converted to cyclopentadienyl radicals and in subsequent steps to smaller hydrocarbons. Alternatively, the initial hydrogen abstraction on the toluene molecule can occur at the ring, leading to methyl phenyl radicals. These are oxidized to benzoquinone. The main reaction pathways in all flames in the simulation with the reaction mechanism of Shao et al. [6] do not differ substantially from the mechanism of Yuan et al. [5]. The main differences are that the oxidation of the benzyl radical to benzaldehyde is of less importance in the Shao et al. [6] mechanism, and ortho-benzoquinone is not formed. Instead, methyl-phenyl radicals which are formed from toluene by hydrogen abstraction attach oxygen to the ring in a reaction with molecular oxygen, and decompose assisted by H atoms to phenyl radicals and CO. Only in the Yuan et al. [5] mechanism, peroxybenzene is formed in a reaction of phenyl radicals with oxygen, while the Shao et al. [6] mechanism only contains reactions going to phenyloxy radicals. In their recent paper Morozov et al. [30] discuss that collisional stabilization of peroxybenzene competes with the bimolecular product channels to phenoxy + O and 2,4-cyclopentadienone + HCO at temperatures below 1500 K and pressures above 1 bar. Both reaction channels appear reasonable at the low temperatures in the flame front in low-pressure flames. With 1200 K the temperature in flame C is low enough in the simulation with the Yuan et al. [5] mechanism for the formation of peroxybenzene. The peroxybenzene is also found in the simulations with this mechanism of flames A and B as another important intermediate, even though the flame temperatures are significantly higher (1500 K and 1350 K, respectively). In the PEPICO measurements no signal appeared at $m/z = 109$ which would correspond to the peroxybenzene. In addition, the photoionization energy of cyclopentadienone near 9.5 eV [31] is higher than the highest recorded photon energy for our ms-TPES, so that our data remain inconclusive to this issue. Very noisy signal at $m/z = 110$ could indicate the presence of very small amounts of phenyl hydroperoxide. Compared to the methylperoxy radical the formation of phenylperoxy radical is similarly fast, but the reverse reaction in this temperature range is slower. Methylperoxy radicals were detected in the flame front of comparable laminar low-pressure flames by Bierkandt et al. [32].

The cyclopentadienyl radicals can react with acetylene to give fulvenallene, initiating further reactions via five-membered-ring species. The predicted reaction pathways in both mechanisms are plausible, and several of the predicted intermediates are detected experimentally and identified by their photoionization properties.

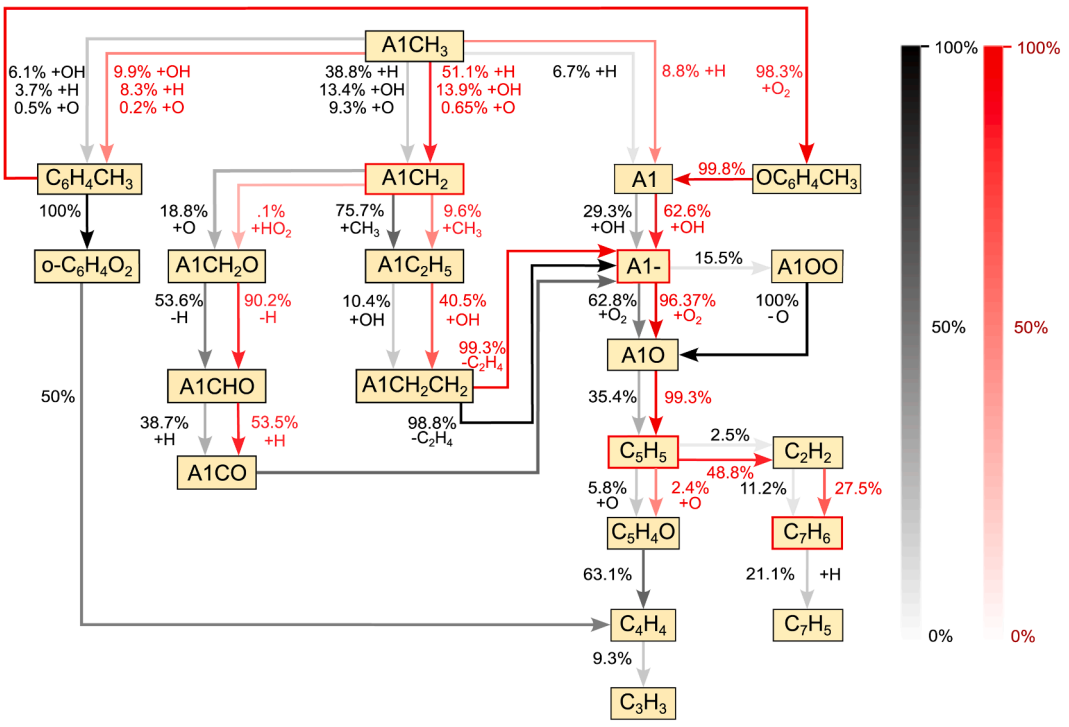

Fig. 3. Reaction pathways of toluene consumption in Flame A at HAB=6.5mm. Percentages and arrows in grey shades signify the carbon flux relative to the total carbon flux though this species simulated with reaction mechanism of Yuan et al. [5]. Red color denotes the same properties for the simulation with the mechanism of Shao et al. [6].

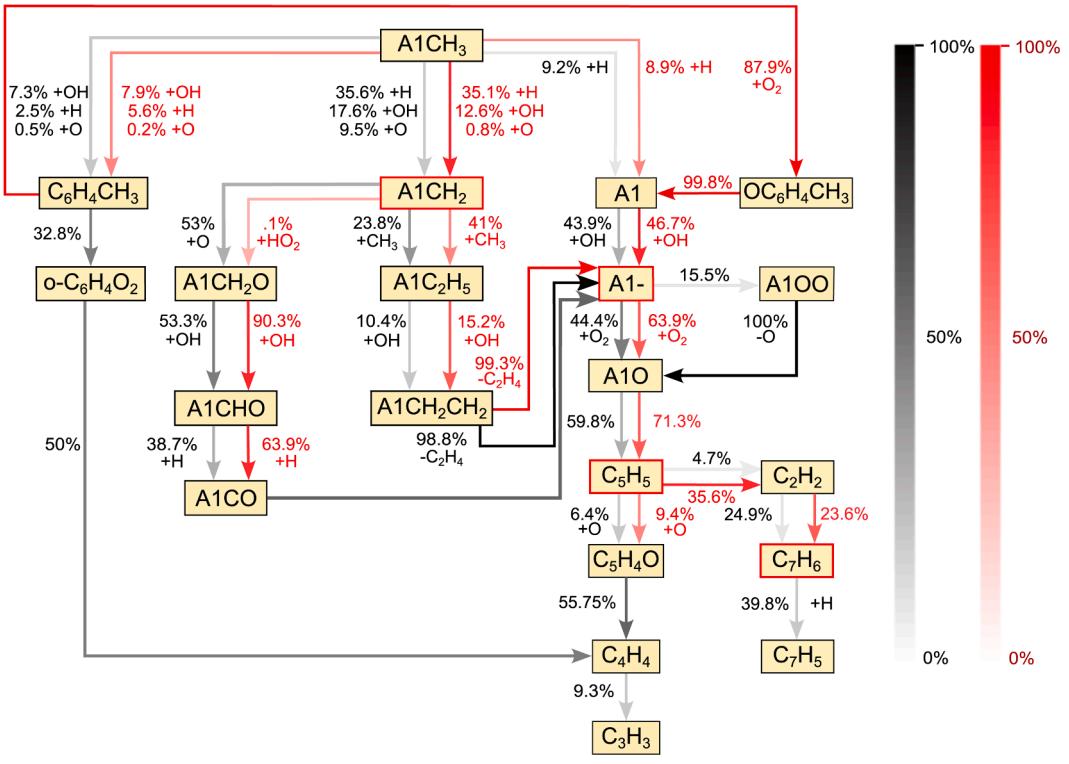

Fig. 4. Reaction pathways of toluene consumption in Flame B at HAB=6.5mm. Percentages and arrows in grey shades signify the carbon flux relative to the total carbon flux though this species simulated with reaction mechanism of Yuan et al. [5]. Red color denotes the same properties for the simulation with the mechanism of Shao et al. [6].

The benzyl radical is clearly identified by comparison to the ms-TPES of the benzyl radical measured by Savee et al. [33] in all flames investigated here (Fig. 6a). Similarly, ethylbenzene can be assigned unambiguously as the most abundant species to the ms-TPES recorded for the species at a mass-to-charge ratio (m/z) of 106. m- and o-xylene are also present in smaller amounts as can be seen from signal below the

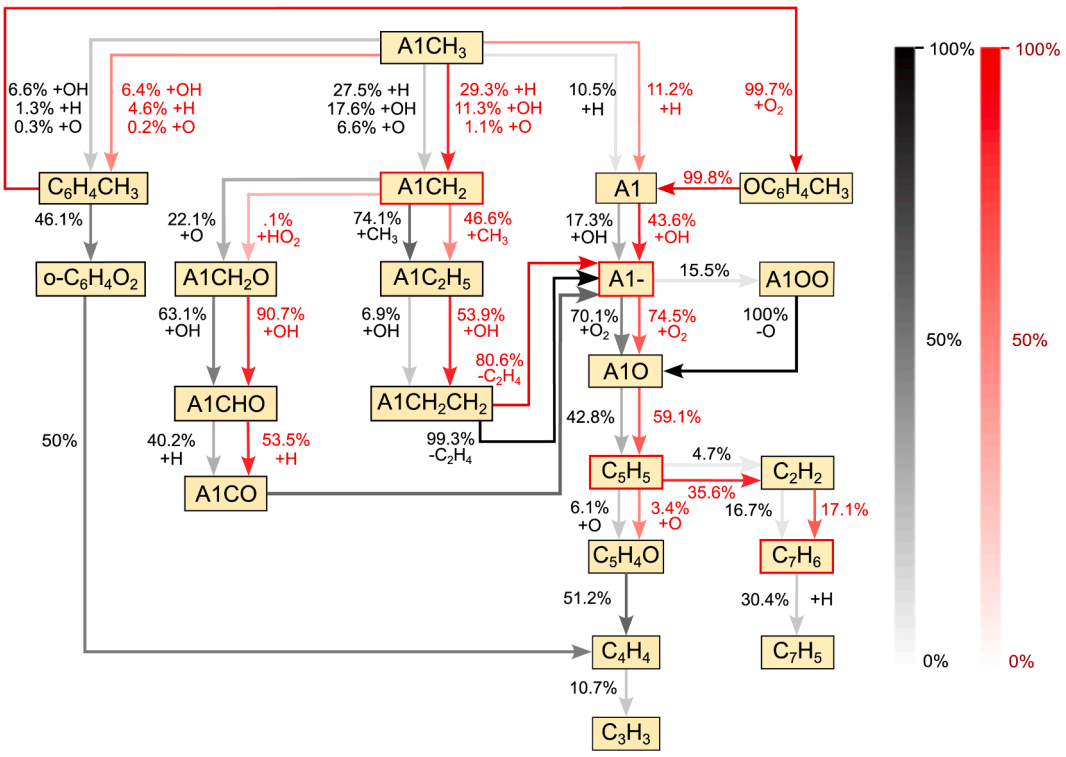

Fig. 5. Reaction pathways of toluene consumption in Flame C at HAB=6.5mm. Percentages and arrows in grey shades signify the carbon flux relative to the total carbon flux though this species simulated with reaction mechanism of Yuan et al. [5]. Red color denotes the same properties for the simulation with the mechanism of Shao et al. [6].

ionization energy of ethylbenzene of 8.77 eV [34] and above 8.55 eV [34] and 8.56 eV [34] for m- and o-xylene, respectively (Fig. 7). The phenylethyl radical is not detected by either ms-TPES or PIE curve for $m/z = 105$ because its ionization energy (6.9 eV [34]) is expected to be below the starting energy of the energy scan of 7 eV.

The phenyl radical is detected by the PIE curve measured for $m/z = 77$ in Fig. 6b in flames B and C. The ionization energy of the phenyl radical of 8.32 eV [35] matches the onset in the PIE curve. Unfortunately, the signal-to-noise ratio of the ms-TPES is insufficient for species identification. The same applies to the phenoxy radical or the peroxybenzene.

The cyclopentadienyl radical is detected in all flames and the reaction pathway to fulvenallene is corroborated by the presence of the fulvenallene, assigned by its ms-TPES at $m/z = 65$ and $m/z = 90$ shown in Fig. 6c and d, respectively. In Fig. 6c the ionization energy of the cyclopentadienyl radical of 8.41 eV [36] is clearly visible in the first transition of the spectrum. In Fig. 6d vibrational progressions of at least two different species can be seen. The second peak at 8.27 eV corresponds to the ionization energy of the fulvenallene [37]. We calculated the ionization energies of other C_7H_6 isomers using CBS-QB3 methods with Gaussian, and cyclo-C_7H_6, and singlet or triplet phenylcarbene with ionization energies of 7.63 eV, 7.29 eV and 7.41 eV, respectively, could be responsible for the first peak. Neither the ms-TPES (Fig. 6e) nor the PIE curve at $m/z = 108$ show any traces of 1,4-benzoquinone in all flames. This could be an indication that the mechanism of Yuan et al. [5] overestimates these mole fractions.

3.4. *Influence of acetylene and 1,3-butadiene on toluene consumption in the flame front*

The increase in toluene consumption in the flame front of the doped flames is caused by the conversion of the added fuel. To understand the influence of the additives on the toluene oxidation, their reaction pathways in the flame front must be analyzed. Fig. 8 shows a reaction pathway analysis of 1,3-butadiene consumption in the flame front at HAB=3.5 mm.

In agreement with the experimental observation that 1,3-butadiene oxidation starts before significant oxidation of toluene sets in, hydrocarbon intermediates formed in the toluene decomposition do not influence the consumption pathway of 1,3-butadiene. At the low temperature of 560 K in flame B at this position, 1,3-butadiene consumption is initiated by hydrogen addition to a terminal methyl group giving the SAX-C_4H_7 radical. Both reaction mechanisms agree on this step. The hydrogen atom is formed either in reactions of 1,3-butadiene with oxygen or transported upstream via diffusion. In the Yuan et al. mechanism [5], the SAX-C_4H_7 radical stabilizes by hydrogen addition to 1- and 2-butene. All three species react to propene and subsequently ethylene and vinyl radicals. Oxidation occurs via methylperoxide and methoxy radicals. Alternatively, SAX-C_4H_7 reacts to methane and is oxidized via methanol and CH_2O. In the simulations with the Shao et al. [6] mechanism SAX-C_4H_7 is oxidized predominantly by reaction with HO_2 to C_4H_7O, which in turn reacts via vinyl or methoxy radicals to formaldehyde.

Fig. 9 presents the reaction path analysis of acetylene with the Yuan et al. [5] mechanism. For acetylene, fuel consumption at HAB=3.5 mm with a temperature of 590 K in the flame starts mainly by hydrogen addition to the fuel yielding vinyl radicals. Only 20% of the acetylene are oxidized to ketenyl radicals by reactions with the small flame radicals H and O. The vinyl radical reacts to HCO. In the direct reaction some acetylene is reformed. Along the other reaction pathways oxidation occurs stepwise in reactions with mainly O and HO_2.

The reaction path analysis of acetylene with the reaction mechanism of Shao et al. [6] is presented in Fig. 9. Here, oxidation to ketenyl radicals is with 80% the most important pathway, while the hydrogen addition to acetylene to yield vinyl radicals has much smaller carbon flux than in the simulation with the Yuan et al. [5] mechanism. Despite the difference in the initial reaction step, the subsequent reaction pathways remain similar. An influence of hydrocarbon intermediates

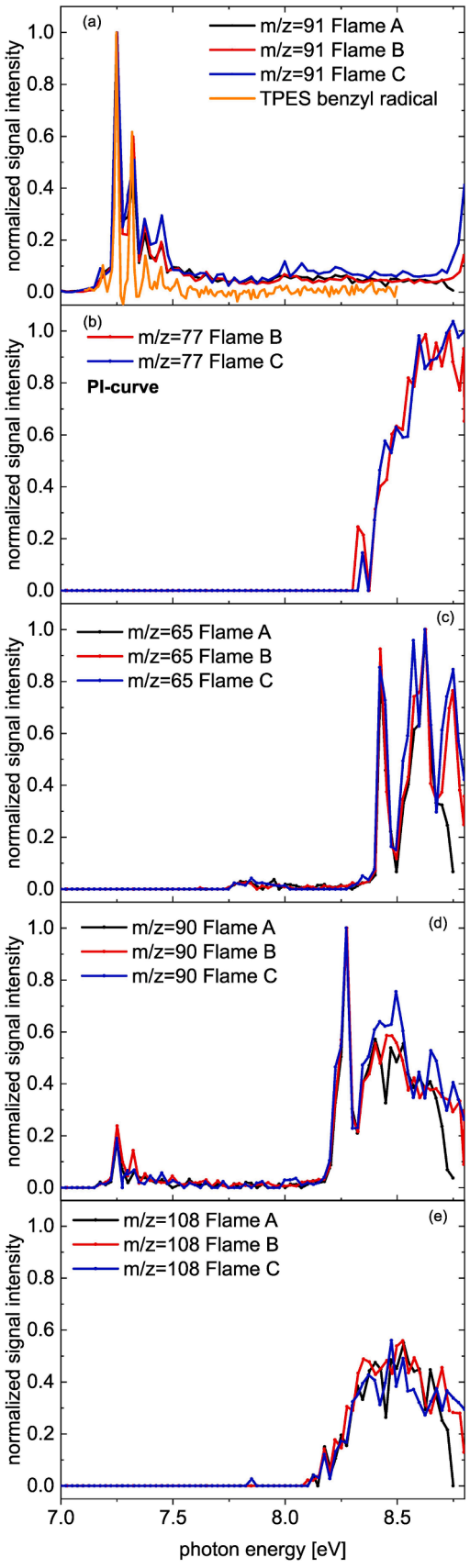

(caption on next column)

Fig. 6. a) ms-TPES of $m/z = 91$ in Flames A-C with an onset at the ionization energy of the benzyl radical – literature TPES: [33], b) PIE curve of $m/z = 77$ in Flame B and C with a transition at the ionization energy of the phenyl radical – literature PI-curve: [38], c) ms-TPES of $m/z = 65$ in Flames A-C with a transition at the ionization energy of the cyclopentadienyl radical – literature TPES: [39], d) ms-TPES of $m/z = 90$ in Flames A-C with a transition at the ionization energy of the fulvenallene at 8.41 eV and evidence of a second isomer – literature TPES: [37], e) ms-TPES of $m/z = 108$.

from toluene conversion is not obvious for either reaction mechanism.

In summary, the reaction path analysis of both fuel dopants shows that there is no large accelerating effect of toluene on the oxidation of the additive. Also, inspite of differences in the fuel conversion pathways of the additive, both reaction mechanisms lead to similar predictions of the fuel conversion of each additive.

The main reaction pathways of toluene in Flame C at HAB=3.5 mm and HAB=6.5 mm are almost identical and are also very similar in Flame A and B, but overall toluene conversion is low. A rate of production analysis of toluene decomposition at HAB=3.5 mm in Flames A, B and C was performed with both reaction mechanisms. For the reaction mechanism of Yuan et al. [5] it shows that hydrogen abstraction from toluene by H atoms is the most important reaction. The same is true in Flame A (see Fig. S1 in SI). In Flame B, the toluene at this position is consumed mostly through H abstraction by OH radicals as shown in Fig. S2. in SI. However, at the low temperatures in all flames at HAB=3.5 mm the reaction rates of OH radicals and O- and H-atoms with toluene are also very similar.

The analysis using the reaction mechanism of Shao et al. [6] leads to the same conclusions. The only difference between the analyses with the two mechanisms is that the total ROP is higher in all flames using the Shao et al. [6] mechanism. This observation is reflected in the small shift of the species profiles towards the burner mentioned above.

Consequently, different overall levels of small flame radicals will increase toluene reactivity. In all flames the radical mole fractions could not be measured. In the simulations the mole fractions of these small radicals are much higher in the two flames with additives at large distances from the burner. At HAB=3.5 mm, where the deviations in reactivity are observed, the mole fractions of H, O, and OH in all flames are very small. This indicates that radicals which are formed in fuel consumption reactions or diffuse to this position in the flame are rapidly consumed again.

We performed a sensitivity analysis for H and OH at HAB=3.5 mm with both mechanisms. These are shown for Flames A and B in Figs. 10 and 11. In flame C, both radicals are consumed in reactions with toluene. In flame B simulated with the reaction mechanism of Yuan et al. [5], OH radicals are produced by reactions of intermediates formed from 1, 3-butadiene and they are mainly consumed in the decomposition reactions of toluene, and in reactions involving methyl radicals. The methyl radicals are mostly formed in 1,3-buatdiene decomposition. The H atom on the other hand is consumed mostly in reactions of 1,3-butadiene intermediates and contributes less to toluene decomposition (see Fig. 10).

The simulation with the mechanism of Shao et al. [6], shown in Fig. 10 (right side) leads to the same observations. In both mechanisms the most sensitive reaction for H atom consumption is the reaction of the SAX-C_4H_7 radical to the stable species C_4H_6 by loss of a H atom. So, one aspect in 1,3-butadiene decomposition is the formation of resonantly stabilized radicals, which consume OH radicals and H atoms when they react to even more stable hydrocarbons. The most sensitive reaction for OH consumption is in both mechanisms the hydrogen abstraction by OH from toluene. The relevance of other OH and H producing and consuming reactions varies slightly.

In flame A simulated by the reaction mechanism of Yuan et al. [5], H atoms as well as OH radicals are formed through reactions of intermediates arising from acetylene consumption with the vinyl radical being the most important intermediate in this respect. In contrast to

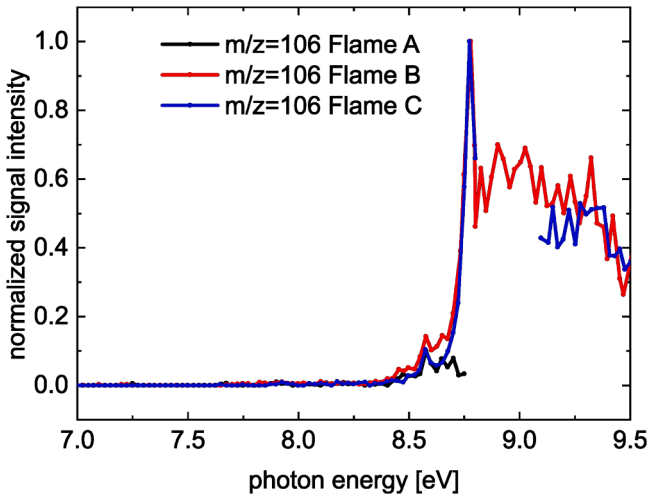

Fig. 7. ms-TPES of $m/z = 106$ in Flames A-C with a transition at the ionization energy of the ethylbenzene at 8.77 eV and a transition at the ionization energy of m- and o-xylene at 8.55 eV and 8.56 eV.

Flame B both, H and OH, are consumed mostly in toluene conversion as can be seen in Fig. 11. Again, the same observations are found for the simulation with the Shao et al. mechanism [6]. Using both mechanisms, the reactions of H atoms with toluene to either phenyl or benzyl radicals are identified as the most sensitive for H and OH consumption, while reactions with less sensitivity differ slightly between the two mechanisms. Acetylene does not form many resonantly stabilized radicals along its consumption pathways, so that OH and H are not consumed in stabilization reactions of these species.

Our interpretation of these findings is as follows: 1,3-butadiene is the most reactive of the three fuels discussed here. While its consumption produces the small flame species that lead to faster toluene consumption in the fuel mixture, it also competes with the toluene for these radicals. Acetylene, which is less reactive than 1,3-butadiene and more reactive than toluene, also enhances toluene consumption in the flame by a similar radical promoted mechanism in the flame front. Because of its lower reactivity, C_2H_2 oxidation itself consumes less of these radicals so that faster decomposition of toluene in the flame front occurs than for 1,3-butadiene. Acetylene is also the smaller hydrocarbon and strongly exothermic reaction sequences leading from the fuel to small intermediates such as HCO and CO require fewer reaction steps and fewer small radicals so that more heat is released in the flame front. This circumstance leads to the observed steeper increase of the flame temperature in flame A.

4. Conclusions

Addition of 1,3-butadiene and acetylene to toluene fuel in laminar flat flames leads to a faster consumption of toluene. This sensitizing effect is mediated exclusively through the small flame species H, O and OH and not through hydrocarbon intermediates formed from either fuel. This observation differs from results of pyrolysis studies where no oxygen is present and radical levels are typically much lower, because reactions are induced by external heating. Under these conditions an accelerating effect was explained by the production of H radicals through a reaction of the benzyl radical with C_2H_x intermediates [7,11]. Also, under the flame conditions investigated here, the more reactive fuel additive, 1,3-butadiene, increases toluene reactivity in the flame front to a lower extent than the less reactive fuel additive, acetylene. We could trace these differences to a competition between the production of OH and H by the consumption of the additive, and the consumption of these small species by the oxidation of the additive itself.

Overall, the reaction mechanisms of Yuan et al. [5] and Shao et al. [6] that were used for the analysis show good agreement with the experimental data. In particular, the toluene decomposition pathways were supported by identification of major intermediates by ms-TPES and PIE curves. The reaction pathways predicted by the two mechanisms differ in details in particular for toluene and 1,3-butadiene consumption steps. Here, a comparison to a more detailed analysis of intermediate

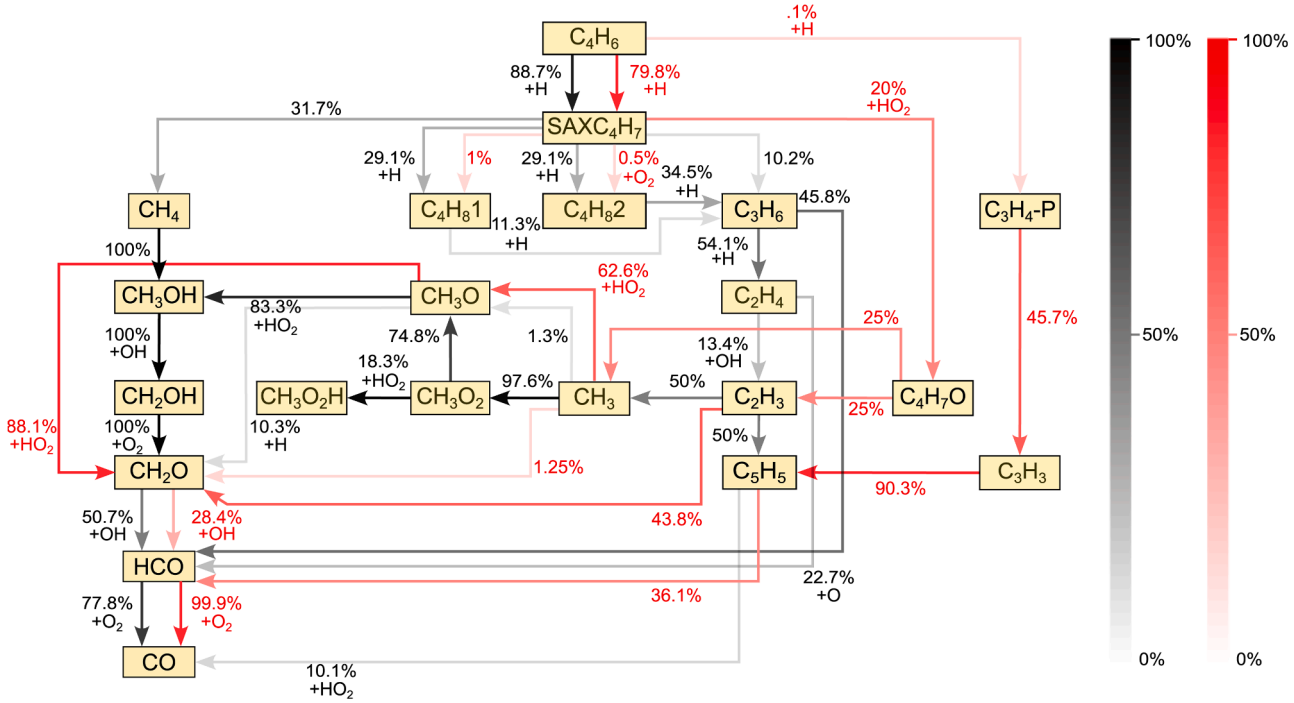

Fig. 8. Reaction pathways of 1,3-butadiene consumption in Flame B at HAB=3.5mm. Percentages and arrows in grey shades signify the carbon flux relative to the total carbon flux though this species with the Yuan et al. mechanism, while percentages and arrows in red shades were obtained with the mechanism of Shao et al. [6].

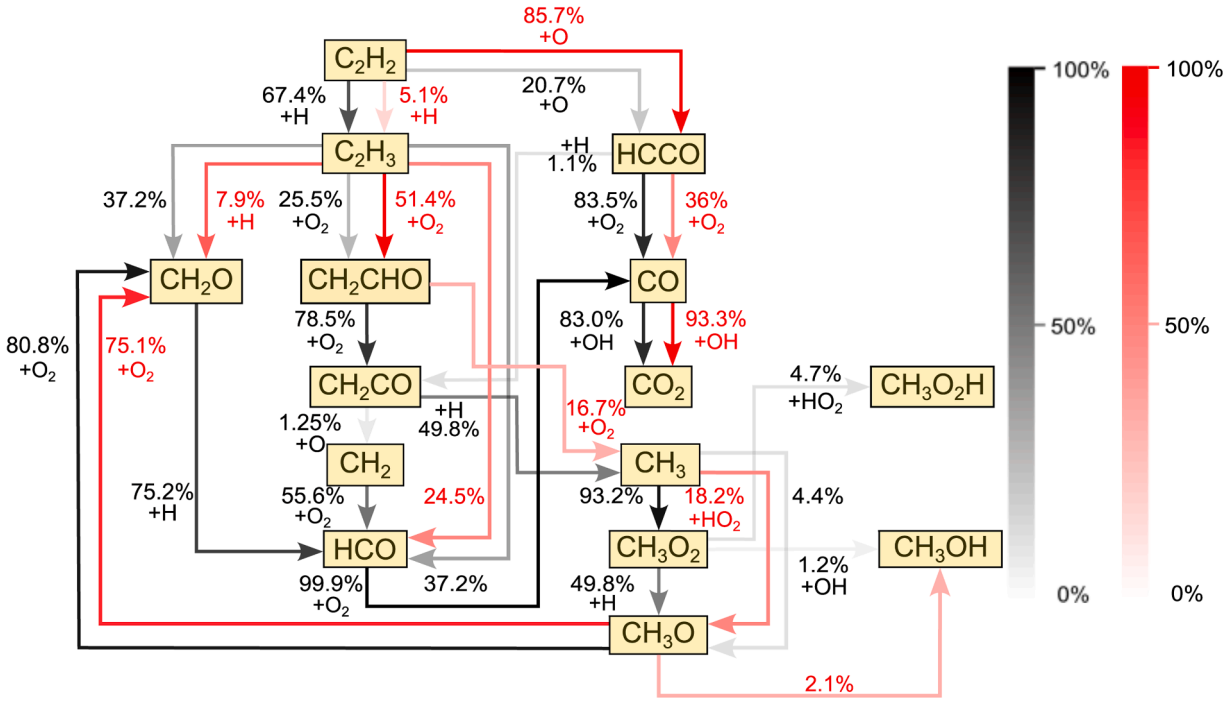

Fig. 9. Reaction pathways of acetylene consumption in Flame A at HAB=3.5mm. Percentages and arrows in grey shades signify the carbon flux relative to the total carbon flux though this species with the Yuan et al. mechanism, while percentages and arrows in red shades were obtained with the mechanism of Shao et al. [6].

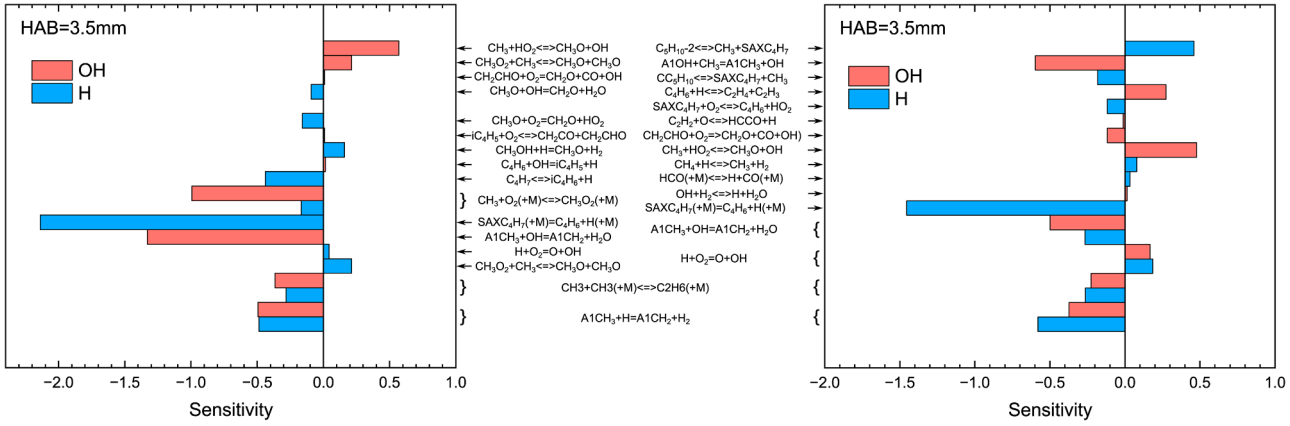

Fig. 10. Sensitivity analysis of OH and H forming and consuming reactions at HAB=3.5 mm in Flame B. Left: Yuan et al. [5] – Right: Shao et al. [6].

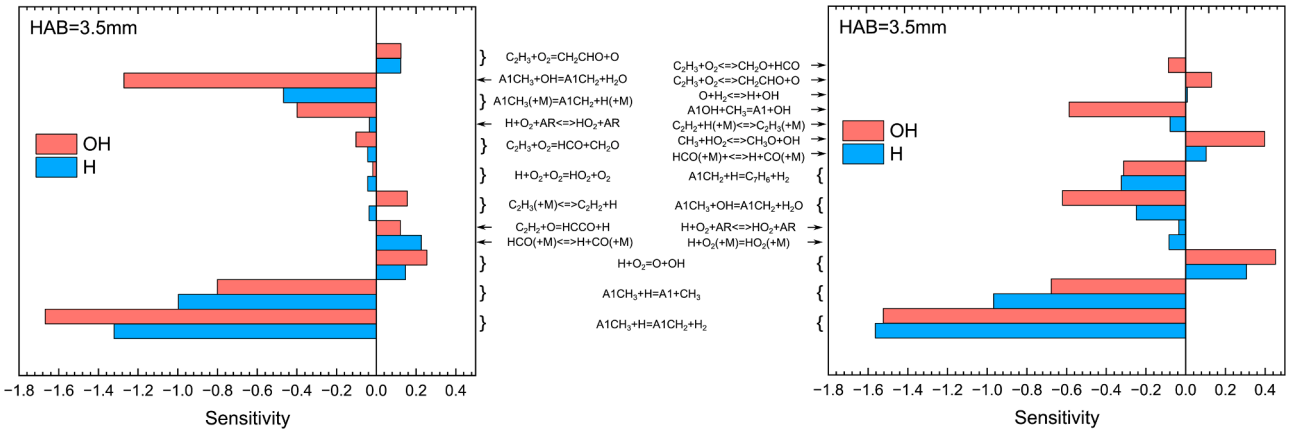

Fig. 11. Sensitivity analysis of OH and H forming and consuming reactions at HAB=3.5 mm in Flame A. Left: Yuan et al. [5] – Right: Shao et al. [6].

species profiles in future work may lead to a better assessment of the correctness of the pathways. For the analysis of the observed reactivity differences of the fuel mixtures, both mechanisms are highly suitable for analyzing the intricate interaction of different fuel components in flames containing toluene and lead to the same conclusions.

Novelty and Significance Statement

The chemical kinetic interaction of different fuel components is of interest in the context of reference fuel design and mixture reactivity in chemically controlled ignition. The novelty of this research is an explanation for the experimental observation that in laminar toluene flames, the more reactive fuel additive, butadiene, increases the toluene reactivity in the flame front to a lower extend than the less reactive fuel additive, acetylene. We find that a competition between the production of OH and H by the consumption of the additive, and the consumption of these small species by the oxidation of the additive itself, shape the overall reactivity of the mixture. The finding is significant because it raises awareness that simple rules, i.e., "the more reactive additive leads to the more reactive mixture" cannot predict the mixture reactivity under flame conditions.

CRediT authorship contribution statement

Ewald Keksel: Writing – original draft, Visualization, Data curation. **Sebastian Kluge:** Data curation. **Domenik Schleier:** Formal analysis. **Martin Höner:** Data curation. **Yasin Karakaya:** Data curation. **Thomas Bierkandt:** Data curation, Conceptualization. **Markus Köhler:** Funding acquisition, Data curation, Conceptualization. **Tina Kasper:** Writing – original draft, Supervision, Funding acquisition, Formal analysis, Data curation, Conceptualization.

Declaration of competing interest

The authors declare that they have no known competing financial interests or personal relationships that could have appeared to influence the work reported in this paper

Acknowledgements

The authors are thankful for beamtime and support by Patrick Hemberger, Andras Bodi and Domenik Krüger at the SLS. Funding by the Helmholtz Association is acknowledged by T.B. and M.K. Funding by the DFG under contracts 270672969 and 277012063 is gratefully acknowledged.

Supplementary materials

Supplementary material associated with this article can be found, in the online version, at doi:10.1016/j.combustflame.2025.113978.

References

[1] E. Nuss, M. Wick, J. Andert, J. de Schutter, M. Diehl, D. Abel, T. Albin, Nonlinear model predictive control of a discrete-cycle gasoline-controlled auto ignition engine model: simulative analysis, Int. J. Engine Res. 20 (2019) 1025–1036.
[2] M. Korkmaz, R. Zweigel, B. Jochim, J. Beeckmann, D. Abel, H. Pitsch, Triple-injection strategy for model-based control of premixed charge compression ignition diesel engine combustion, Int. J. Engine Res. 19 (2018) 230–240.
[3] S. Dong, S.W. Wagnon, L. Pratali Maffei, G. Kukkadapu, A. Nobili, Q. Mao, M. Pelucchi, L. Cai, K. Zhang, M. Raju, T. Chatterjee, W.J. Pitz, T. Faravelli, H. Pitsch, P.K. Senecal, H.J. Curran, A new detailed kinetic model for surrogate fuels: C3MechV3.3, Appl. Energy Combust. Sci. 9 (2022) 100043.
[4] J. Andrae, Comprehensive chemical kinetic modeling of toluene reference fuels oxidation, Fuel 107 (2013) 740–748.
[5] W. Yuan, Y. Li, P. Dagaut, J. Yang, F. Qi, Investigation on the pyrolysis and oxidation of toluene over a wide range conditions. II. A comprehensive kinetic modeling study, Combust. Flame 162 (2015) 22–40.
[6] C. Shao, H. Wang, N. Atef, Z. Wang, B. Chen, M. Almalki, Y. Zhang, C. Cao, J. Yang, S.M. Sarathy, Polycyclic aromatic hydrocarbons in pyrolysis of gasoline surrogates (n-heptane/iso-octane/toluene), Proc. Combust. Inst. 37 (2019) 993–1001.
[7] W. Sun, A. Hamadi, S. Abid, N. Chaumeix, A. Comandini, Detailed experimental and kinetic modeling study of toluene/C2 pyrolysis in a single-pulse shock tube, Combust. Flame 226 (2021) 129–142.
[8] S.G. Davis, H. Wang, K. Breinsky, C.K. Law, Laminar flame speeds and oxidation kinetics of benene-air and toluene-air flames, Symp. Int. Combust. Proc. 26 (1996) 1025–1033.
[9] S.S. Vasu, D.F. Davidson, R.K. Hanson, Shock-Tube experiments and kinetic modeling of toluene ignition, J. Propul. Power 26 (2010) 776–783.
[10] P. Dagaut, G. Pengloan, A. Ristori, Oxidation, ignition and combustion of toluene: experimental and detailed chemical kinetic modeling, Phys. Chem. Chem. Phys. 4 (2002) 1846–1854. http://www.rsc.org/suppdata/cp/b1/b110282f.
[11] T. Li, Y. Zhang, W. Yuan, C. Cao, W. Li, J. Yang, Y. Li, Unraveling synergistic effects on pyrolysis reactivity and indene formation in co-pyrolysis of toluene and acetylene, Proc. Combust. Inst. 38 (2021) 1413–1421.
[12] Y. Li, J. Cai, L. Zhang, T. Yuan, K. Zhang, F. Qi, Investigation on chemical structures of premixed toluene flames at low pressure, Proc. Combust. Inst. 33 (2011) 593–600.
[13] Z. Tian, W.J. Pitz, R. Fournet, P.-A. Glaude, F. Battin-Leclerc, A detailed kinetic modeling study of toluene oxidation in a premixed laminar flame, Proc. Combust. Inst. 33 (2011) 233–261.
[14] Y. Zhang, K.P. Somers, M. Mehl, W.J. Pitz, R.F. Cracknell, H.J. Curran, Probing the antagonistic effect of toluene as a component in surrogate fuel models at low temperatures and high pressures. A case study of toluene/dimethyl ether mixtures, Proc. Combust. Inst. 36 (2017) 413–421.
[15] N. Slavinskaya, A. Mirzayeva, R. Whitside, J. Starke, M. Abbasi, M. Auyelkhankyzy, V. Chernov, A modelling study of acetylene oxidation and pyrolysis, Combust. Flame 210 (2019) 25–42.
[16] N. Lokachari, U. Burke, A. Ramalingam, M. Turner, R. Hesse, K.P. Somers, J. Beeckmann, K.A. Heufer, E.L. Petersen, H.J. Curran, New experimental insights into acetylene oxidation through novel ignition delay times, laminar burning velocities and chemical kinetic modelling, Proc. Combust. Inst. 37 (2019) 583–591.
[17] C.-W. Zhou, A. Farooq, L. Yang, A.M. Mebel, Combustion chemistry of alkenes and alkadienes, Prog. Energy Combust. Sci. 90 (2022) 100983.
[18] C.-W. Zhou, Y. Li, U. Burke, C. Banyon, K.P. Somers, S. Ding, S. Khan, J.W. Hargis, T. Sikes, O. Mathieu, E.L. Petersen, M. AlAbbad, A. Farooq, Y. Pan, Y. Zhang, Z. Huang, J. Lopez, Z. Loparo, S.S. Vasu, H.J. Curran, An experimental and chemical kinetic modeling study of 1,3-butadiene combustion: ignition delay time and laminar flame speed measurements, Combust. Flame 197 (2018) 423–438.
[19] H.A. Gueniche, P.A. Glaude, R. Fournet, F. Battin-Leclerc, Rich premixed laminar methane flames doped by light unsaturated hydrocarbons, Combust. Flame 151 (2007) 245–261.
[20] Z. Wan, L. Shi, D. Chen, P. Li, C. Zhang, Experimental and kinetic study of the effects of n-butanol addition on toluene reference fuel auto-ignition, Fuel 337 (2023) 126858.
[21] T. Javed, C. Lee, M. AlAbbad, K. Djebbi, M. Beshir, J. Badra, H. Curran, A. Farooq, Ignition studies of n-heptane/iso-octane/toluene blends, Combust. Flame 171 (2016) 223–233.
[22] D. Kaczmarek, B. Atakan, T. Kasper, Investigation of the partial oxidation of methane/n-heptane-mixtures and the interaction of methane and n-heptane under ultra-rich conditions, Combust. Flame 205 (2019) 345–357.
[23] S. Porras, D. Kaczmarek, J. Herzler, S. Drost, M. Werler, T. Kasper, M. Fikri, R. Schießl, B. Atakan, C. Schulz, U. Maas, An experimental and modeling study on the reactivity of extremely fuel-rich methane/dimethyl ether mixtures, Combust. Flame 212 (2020) 107–122.
[24] P. Osswald, P. Hemberger, T. Bierkandt, E. Akyildiz, M. Köhler, A. Bodi, T. Gerber, T. Kasper, In situ flame chemistry tracing by imaging photoelectron photoion coincidence spectroscopy, Rev. Sci. Instrum. 85 (2014) 25101.
[25] T. Bierkandt, P. Hemberger, P. Oßwald, M. Köhler, T. Kasper, Insights in m-xylene decomposition under fuel-rich conditions by imaging photoelectron photoion coincidence spectroscopy, Proc. Combust. Inst. 36 (2017) 1223–1232.
[26] T.A. Cool, K. Nakajima, C.A. Taatjes, A. McIlroy, P.R. Westmoreland, M.E. Law, A. Morel, Studies of a fuel-rich propane flame with photoionization mass spectrometry, Proc. Combust. Inst. 30 (2005) 1681–1688.
[27] Y. Karakaya, J. Sellmann, I. Wlokas, T. Kasper, Influence of the sampling probe on flame temperature, species, residence times and on the interpretation of ion signals of methane/oxygen flames in molecular beam mass spectrometry measurements, Combust. Flame 229 (2021) 111388.
[28] L. Zhang, J. Cai, T. Zhang, F. Qi, Kinetic modeling study of toluene pyrolysis at low pressure, Combust. Flame 157 (2010) 1686–1697.
[29] S. Park, Y. Wang, S.H. Chung, S.M. Sarathy, Compositional effects on PAH and soot formation in counterflow diffusion flames of gasoline surrogate fuels, Combust. Flame 178 (2017) 46–60.
[30] A.N. Morozov, I.A. Medvedkov, V.N. Azyazov, A.M. Mebel, Theoretical study of the phenoxy radical recombination with the O(3P) atom, phenyl plus molecular oxygen revisited, J. Phys. Chem. A. 125 (2021) 3965–3977.
[31] D.S.N. Parker, R.I. Kaiser, T.P. Troy, O. Kostko, M. Ahmed, A.M. Mebel, Toward the oxidation of the phenyl radical and prevention of PAH formation in combustion systems, J. Phys. Chem. A. 119 (2015) 7145–7154.
[32] T. Bierkandt, P. Oßwald, N. Gaiser, D. Krüger, M. Köhler, M. Hoener, S. Shaqiri, D. Kaczmarek, Y. Karakaya, P. Hemberger, T. Kasper, Observation of low-temperature chemistry products in laminar premixed low-pressure flames by molecular-beam mass spectrometry, Int. J. Chem. Kinet. 53 (2021) 1063–1081.

[33] J.D. Savee, J. Zádor, P. Hemberger, B. Sztáray, A. Bodi, D.L. Osborn, Threshold photoelectron spectrum of the benzyl radical, Mol. Phys. 113 (2015) 2217–2227.
[34] P. Linstrom, NIST chemistry WebBook, in: NIST Standard Reference Database 69, 1997.
[35] V. Butcher, M.L. Costa, J.M. Dyke, A.R. Ellis, A. Morris, A study of the phenyl radical by vacuum ultraviolet photoelectron spectroscopy, Chem. Phys. 115 (1987) 261–267.
[36] N. Hansen, S.J. Klippenstein, J.A. Miller, J. Wang, T.A. Cool, M.E. Law, P. R. Westmoreland, T. Kasper, K. Kohse-Höinghaus, Identification of C5Hx isomers in fuel-rich flames by photoionization mass spectrometry and electronic structure calculations, J. Phys. Chem. A. 110 (2006) 4376–4388.
[37] M. Steinbauer, P. Hemberger, I. Fischer, A. Bodi, Photoionization of C7H6 and C7H5: observation of the fulvenallenyl radical, ChemPhysChem 12 (2011) 1795–1797.
[38] N.E. Sveum, S.J. Goncher, D.M. Neumark, Determination of absolute photoionization cross sections of the phenyl radical, Phys. Chem. Chem. Phys. PCCP 8 (2006) 592–598.
[39] P. Hemberger, G.Da Silva, A.J. Trevitt, T. Gerber, A. Bodi, Are the three hydroxyphenyl radical isomers created equal?–The role of the phenoxy radical, Phys. Chem. Chem. Phys. 17 (2015) 30076–30083.